ROYAL SOCIETY
OF CHEMISTRY

PAPER

Check for updates

Kinetic and thermodynamic characterization of thermosonication-assisted extraction of bioactives from lapsi fruit juice optimized by ANN-GA

Puja Das,[ab] Prakash Kumar Nayak[a] and Radha krishnan Kesavan ![ORCID] *[a]

The present study focuses on an extensive investigation into thermosonication as a novel process for enhancing the extraction of bioactive functional compounds from lapsi fruit juice. Process optimization was achieved by using artificial neural networks (ANN) coupled with a genetic algorithm (GA), finding optimum conditions to be 75% amplitude, 40 °C, and 60 minutes. The release performance of principal functional compounds, such as total phenolic content, total flavonoid content, antioxidant activity, and ascorbic acid, was also investigated under these optimized conditions. Among all the kinetic models used, the pseudo-second-order model demonstrated the best correlation ($R^2 = 0.99$, $\chi^2 = 0.09$), which indicated that compound release occurred by chemisorption processes. The process also revealed an initial rapid extraction phase, which was then followed by a steady plateau at 60 minutes. The activation energies were in the range of 29.45 to 35.23 kJ mol^{-1}, and this indicated the temperature dependence of the process. Thermodynamic studies revealed that the extraction was spontaneous under all tested temperatures (ΔG: −5.45 to −18.46 kJ mol^{-1}), endothermic in nature (ΔH: 5.44 to 15.64 kJ mol^{-1}), entropy-guided (ΔS: 18.03 to 57.23 J mol^{-1} K^{-1}) and, therefore, capable of efficiently breaking down the cell walls and facilitating mass transfer. Optimal extraction efficiency was achieved at 40 °C, beyond which heat-induced degradation of labile compounds was observed. Kinetic and thermodynamic studies confirm that thermosonication enables efficient, spontaneous, and temperature-dependent extraction of bioactives from Lapsi juice. The findings support its feasibility for energy-efficient, scalable industrial applications.

Sustainability spotlight

Thermosonication is a new green technology that holds great potential in improving the nutritional and functional values of underutilized fruits, such as lapsi (*Choerospondias axillaris*), by supporting sustainable food processing objectives. Through the employment of synergistic combinations of mild heat and ultrasonic waves, this method supports the effective release of bioactive compounds without degradation, which is usually linked with traditional thermal approaches. Unlike using only high temperatures, thermosonication provides a more gentle and controlled extraction condition, with the added benefit of protecting heat-sensitive nutrients and thus enhancing the total yield. Its use for nutrient extraction from lapsi, a fruit native to Sikkim and the Himalayan hilly regions, highlights its potential in unearthing the value of non-conventional plant resources that are often underutilized because of market or processing constraints. By kinetic and thermodynamic modeling, this work gives better mechanistic insights into the mass transfer behavior, energy demand, and compound stability during processing, which are the factors critical to assessing its potential for industrial scalability. Results show that careful control of parameters like temperature and sonication amplitude is important in achieving maximum efficiency without compromising the product quality. Therefore, this study not only emphasizes the technological strengths of thermosonication but also opens the doors for the widespread implementation of sustainable, nutrient-protecting technologies in food supply chains. Finally, this study promotes the translation of regional biodiversity into viable food innovations that benefit the human health as well as environmental sustainability.

1 Introduction

Thermosonication (TS), which integrates the use of ultrasound with mild thermal treatments, has drawn attention because it can preserve bioactive components, inactivate enzymes, and inactivate bacteria in fruit juices, improving the juice quality while consuming lesser energy than traditional approaches.[1] Despite its many advantages, a deeper comprehension of the fundamental concepts governing the extraction kinetics and thermodynamic laws of thermosonicated juices is still required.[2] Computer simulation studies using ANN-GA and other methods not only bridge the gap between application and maximizing the efficiency but also provide a scientific basis for

[a]Department of Food Engineering & Technology, Central Institute of Technology, Deemed to be University, Kokrajhar, B.T.R. Assam, 783370, India. E-mail: k. radhakrishnan@cit.ac.in; Tel: +91-7002909335

[b]Division of Research and Innovation, Uttaranchal Institute of Technology, Uttaranchal University, Dehradun 248007, Uttarakhand, India

commercial use and scaling up.[3,4] Fruits are essential components of a healthy diet. They have vital vitamins, minerals, and fibers to support general health and well-being. Eating a range of fruits and vegetables has been associated with a decreased risk of coronary artery disease, stroke, and some types of cancer.[5]

A lesser-known fruit, lapsi (*Choerospondias axillaris*), is indigenous to Nepal, Bhutan, and some states of Northeast India, including Arunachal Pradesh, Sikkim, and Assam.[6] The lapsi tree bears tiny, light-greenish blooms at the start of spring, followed by tiny, oval fruits that are around two to three centimeter in diameter. The fruit has a sour, tangy flavor and turns yellow or crimson when it is fully mature. It contains a variety of nutrients (such as dietary fiber, vitamin C, and vitamin A), has several health advantages, and is well-known for its anti-inflammatory, antibacterial and antioxidant qualities.[7] In order to comprehend the improved extraction of bioactive components when heat and ultrasonic waves are applied to plant materials, the complicated topic of extraction kinetics of thermosonicated juices integrates concepts from thermodynamics, mass transport processes, and sonochemistry.[2] To describe the kinetics of thermosonication-based extraction, researchers have used a variety of mathematical models (Table 1). The industrial application of thermosonication technology is greatly advanced by the use of kinetic models,

which allowed for process optimization, better quality control, and economical scale-up strategies for manufacturing excellent, nutrient-rich juices that retain the bioactive substances from fruits and vegetables and offer a prolonged shelf life.[8]

Thermodynamic examination of the thermosonication processes entails important parameters, including enthalpy change (ΔH), entropy change (ΔS), and Gibbs free energy change (ΔG). The change in enthalpy (ΔH) is linked with the energy for breaking and forming bonds during the processes. The change in entropy (ΔS) indicates the increase in molecular disorder because of cell disruption. Gibbs free energy change (ΔG) defines the spontaneity of the extraction process and the equilibrium of the reaction. Furthermore, compared with traditional approaches, thermosonication generally lowers the activation energy (E_a) by 15–30%, thus improving the efficiency of the extraction reactions.[9] Thermodynamics constants exhibit non-Arrhenius behaviour at the water–solid interface where cavitation effects are most noticeable, are proof that thermosonication modifies reaction pathways by offering substitutes with lower energy barriers.[10] In contrast to traditional thermal processing methods, the energy efficacy of thermosonication comes from its capacity to concentrate energy in microscopically precise locations where cell disruption occurs.[11] This results in significantly higher extraction yields despite the lower overall electrical inputs; studies have shown savings in energy

Table 1 Various extraction kinetic models

Model name	Equations	Terms	Reference
Second order model	$\dfrac{\mathrm{d}C_t}{\mathrm{d}t} = k(C_e - C_t)^2$	K is the pseudo-second-order extraction rate constant, C_t is the extract amount at time t (g L^{-1}), and C_e is the equilibrium concentration (g L^{-1})	27
Two-site kinetic model	$\dfrac{M_t}{M_\infty} = 1 - Fe^{-k_1 t} - (1-F)e^{-k_2 t}$	M_t and M_∞ are concentrations of the extracted compound at time t and infinity, F is the fraction of solute released during rapid extraction, $(1-F)$ represents the portion of solute released during slower extraction, and k_1 and k_2 are the first-order rate constants that represent the two stages of the extraction process	28
Peleg's model or hyperbolic model	$C_t = \dfrac{t}{k_1 + k_2 t}$	k_1 is the Peleg's rate constant at the beginning of the extraction, and k_2 is Peleg's capacity constant	29
Fick's model	$1 - \dfrac{M_t}{M_\infty} = \dfrac{6}{\pi^2}\exp\left(\dfrac{-D\pi^2 t}{R^2}\right)$	M_t and M_∞ are concentrations of the extracted compound at time t and infinity, D is the effective diffusion coefficient, and R is the radius	30
Parabolic diffusion model	$y = A_0 + A_1 t^{1/2}$	A_0 is the washing coefficient, which indicates the amount of extract extracted instantaneously; A_1 is the diffusion rate constant	31
First-order reaction model	$\dfrac{\mathrm{d}C_t}{\mathrm{d}t} = k(C_e - C_t)$	K is the first-order extraction rate constant, C_t is the amount extracted at time t (g L^{-1}), and C_e is equilibrium concentration (g L^{-1})	32

consumption of 20–45% while accomplishing similar or better extraction of bioactive substances.[12] Enhancing the power-to-mass ratio, controlling the loss of heat during sound energy conversion, striking a balance between the residence duration and energy intensity, and creating accurate mathematical models that can forecast phase changes and compound stability under various thermosonication conditions are examples of practical thermodynamic factors in industrial applications.[13]

The significance of this research extends beyond lapsi fruit to the broader context of underutilized plant resources. Globally, numerous fruits and vegetables remain under-exploited due to the challenges in processing and market integration. Thermosonication offers a versatile platform to valorize such resources, aligning with the Sustainable Development Goals by reducing the waste, enhancing the nutritional availability, and promoting the biodiversity in food systems.[14] For lapsi, the application of TS not only addresses these goals but also taps into its cultural and economic potential in regions where it is a traditional staple. However, realizing this potential requires a detailed understanding of how TS influences the extraction process at a mechanistic level, which is the focus of this study. Kinetic models, such as the pseudo-second-order model and Fick's diffusion model, have been widely used to describe the solid–liquid extraction in food systems, but their adaptation to TS-processed juices, in which liquid–liquid interactions also play certain roles, remains underexplored.[15] Similarly, thermodynamic analyses have been applied to ultrasound-assisted extraction of phytochemicals from herbs and seeds, revealing endothermic processes with positive entropy changes, but data that are specific to fruit juices under TS conditions are limited.

This study builds directly on the foundation laid by an ANN-GA optimization, extending the investigation to the extraction kinetics and thermodynamics of thermosonicated lapsi juice.[16] Herein, kinetic models such as pseudo-second-order, Peleg's, two-site kinetic, pseudo-first-order, parabolic diffusion, and Fick's models were employed to characterize the extraction rates and patterns, complemented by thermodynamic calculations of ΔH, ΔS, and ΔG to assess process feasibility and compound behavior.[17] The choice of these models is based on their proven applicability in food extraction studies and their ability to capture the complex interplay between ultrasound and heat in TS. The experimental design focuses on a temperature range of 30 °C to 50 °C, with measurements taken at 5 minutes intervals for up to 60 minutes and maintaining the optimized 75% amplitude.

2 Materials and methods

2.1 Sample collection and preparation

Fresh lapsi fruits (*Choerospondias axillaris*) were obtained from the local markets in Ranipool, Sikkim. The fruits were packed in insulated containers at 4 °C to maintain their freshness. The fruits were hand-sorted when they arrived at the laboratory to eliminate damaged and overripe specimens and cleaned with potable water, and juice was extracted using a domestic mixer grinder (brand: Bajaj).

2.2 ANN-genetic optimization

The extraction rates for three outcomes were evaluated at various combinations of temperature and extraction duration. A feedforward backpropagation network with one hidden layer consisting of [X] neurons was used for the optimization which was based on performance metrics. The tansig activation function was used in the hidden layer, and purelin was applied in the output layer. The Levenberg–Marquardt algorithm was employed for training. Following the determination of the optimal processing parameters for TSLJ as per the integrated ANN-GA model (75% amplitude, 40 °C, and 60 minutes), the responses were assessed across a temperature range spanning from 30 °C to 50 °C, with measurements taken at 5 minutes intervals, *i.e.* at 0, 5, 10, 15, 20, 25, 30, 35, 40, 45, 50, 55 and 60 min of the sonication time.[16] The amplitude parameter was maintained at the optimized level determined by the ANN-GA model (75%) during the entire extraction process for the kinetic analysis. The ANN model optimized the conditions for juice extraction among the amplitudes of 50%, 75%, and 100%. Fixing the amplitude at 75% for the extraction kinetics study mitigated the added complexity of changing the amplitude and allowed for a focused investigation into the specific influence of temperature and treatment time on extraction kinetics, which was essential for further process optimization and scale-up.

A mutation rate of 0.02 was applied, introducing small, random alterations to the solutions. This low rate ensured that the population maintained diversity and avoided getting trapped in the local optima, allowing the algorithm to explore beyond the immediate vicinity of current solutions without excessively disrupting the evolutionary progress. The GA iterated over 300 generations, providing ample opportunity for the population to evolve toward an optimal solution.[18]

Given that GA is oriented towards minimizing the fitness function, eqn (1) was minimized to achieve the optimization objective.[19]

$$F = \frac{1}{1 + Y} \tag{1}$$

In the context of GA optimization, Y denotes the juice quality attributes predicted by the ANN model, while F stands for the fitness function.

2.3 Chemicals utilized

The chemicals used in the analysis were of analytical or HPLC grade to ensure the accuracy and reliability. For measuring the total phenolic content (TPC), Folin–Ciocalteu reagent ($\geq$98%, Merck), sodium carbonate (Na_2CO_3, $\geq$99.5%, AR grade), and a gallic acid standard ($\geq$99%, Sigma-Aldrich) were used. For assessing the total flavonoid content (TFC), aluminum chloride ($AlCl_3$, $\geq$98%, AR grade), potassium acetate (CH_3COOK, $\geq$99%, AR grade), methanol ($\geq$99.9%, HPLC grade), and a quercetin standard ($\geq$98%, Sigma-Aldrich) were utilized. Ascorbic acid (AA) content was measured using potassium iodate (KIO_3, $\geq$99.5%, AR grade), potassium iodide (KI, $\geq$99%, AR grade), sulfuric acid (H_2SO_4, 95–98%, AR grade), and a freshly prepared

starch solution as an indicator. The antioxidant activity (AOA) was assessed using DPPH (2,2-diphenyl-1-picrylhydrazyl, ≥95%, Sigma-Aldrich) and methanol (≥99.9%, HPLC grade).

2.4 Total phenolic content (TPC)

TPC was determined using the Folin–Ciocalteu reagent method.[20] 0.5 mL of the juice sample was combined with 2.5 mL of 10% (v/v) Folin–Ciocalteu reagent (≥98%, Merck). The contents were incubated at room temperature for 5 minutes. Then, 2.0 mL of a 7.5% (w/v) solution of sodium carbonate was added to the mixture. The reaction mixture was then stored in the dark at room temperature for 30 minutes. The absorbance at 765 nm was recorded using a UV-Vis spectrophotometer. A calibration curve was plotted using gallic acid, and the values were expressed as milligrams of gallic acid equivalents (mg GAE) per mL of juice.

2.5 Total flavonoid content (TFC)

TFC was determined using the aluminum chloride colorimetric method.[21] 0.5 mL of the juice sample was mixed with 2.0 mL of distilled water and 0.15 mL of a 5% aluminum chloride solution. After 5 minutes of incubation, 0.15 mL of 1 M potassium acetate and 1.2 mL of methanol were added to the mixture. The final volume was adjusted to 5.0 mL with distilled water. The solution was incubated at room temperature in the dark for 30 minutes, and the absorbance was measured at 415 nm using a UV-Vis spectrophotometer. Quercetin was used to construct a standard calibration curve, and the results were expressed as milligrams of quercetin equivalents (mg QE) per mL of juice.

2.6 Ascorbic acid (AA) content

The AA concentration in LJ was analysed using the iodometry method.[22] 10 mL of each juice sample was mixed with 20 mL of 2% hydrochloric acid and filtered through a Whatman No. 1 filter paper to remove the particulates. The clear filtrate was then titrated against a standardized iodine solution (prepared by dissolving potassium iodate (KIO_3) and potassium iodide (KI)) using a freshly prepared 1% starch solution as the indicator. The endpoint was identified by the appearance of a persistent blue-black color. The volume of iodine solution consumed was used to calculate the ascorbic acid content, which was expressed as milligrams of ascorbic acid per 100 mL of juice. All titrations were carried out in triplicate for accuracy.

2.7 Antioxidant activity (AOA)

The AOA of the samples was determined using the DPPH (2,2-diphenyl-1-picrylhydrazyl) radical-scavenging method.[23] A 0.1 mM solution of DPPH was prepared in methanol. In a typical assay, 1.0 mL of the juice sample was mixed with 3.0 mL of the DPPH solution. The mixture was vortexed for 30 seconds and incubated in the dark at room temperature for 30 minutes. The absorbance was measured at 517 nm using a UV-Vis spectrophotometer.

2.8 Extraction kinetics of functional compounds in juice samples during the TS treatment

The pseudo-second-order model, two-site kinetic model, Peleg's model, hyperbolic model, Fick's Model, parabolic diffusion model, and first-order reaction model were used to study the extraction kinetics of various functional compounds (EP), including EP_P (total phenolic content), EP_F (total flavonoid content), EP_A (ascorbic acid), EP_{AOA} (antioxidant activity), EP_{TCC} (total carotenoid content), EP_{TCH} (total chlorophyll content), and EP_{TAC} (total anthocyanin content), retained in LJ during the TS process (Table 1).[24–26]

The pseudo-second-order model proved to be suitable and apparent during the extraction studies of different products.[3,34,38] Eqn (2) presents the kinetic model that was used to calculate the extraction rate of functional compounds in TSLJ.

$$\frac{dy}{dt} = k(S_c - y)^2. \tag{2}$$

where y represents the concentration of the functional compounds in the liquid extract at a specific time t, S_c is the saturation concentration of the functional compounds in the liquid extract and k is the pseudo-second-order rate constant.

Boundary conditions: $y = 0$ at $t = 0$; $y = y$ at $t = t$.

Under these boundary conditions, eqn (3) can be formulated from the pseudo-second-order model given in eqn (2).

$$y = \frac{S_c^2 kt}{1 + S_c kt}. \tag{3}$$

Further, eqn (3) can be simplified into a linear form, as presented in eqn (4)

$$\frac{t}{y} = \frac{1}{h} + \frac{t}{S_c}. \tag{4}$$

where h represents the initial extraction pace as t approaches zero, which is the aggregate of k and S_c. The extraction rate constant (k) is associated with temperature using the Arrhenius equation, as illustrated in eqn (5).

2.9 Activation energy

Activation energy is an important thermodynamic parameter because it is the lowest energy threshold that needs to be surpassed so that a reaction can take place. For thermosonication, the assessment of E_a allowed the estimation of the energy efficiency of the process. A lower activation energy relative to conventional processes means that the ultrasound-enhanced treatment enabled quicker extraction or degradation reactions with a lesser heat input, thereby maintaining quality characteristics and boosting process sustainability.

$$k = k_0 \exp\left(-\frac{E_a}{RT}\right). \tag{5}$$

where E_a is the activation energy and R is the gas constant (8.314 J mol^{-1} K^{-1}). Eqn (5) can be expressed in a linear form, as shown in eqn (6).

$$\ln(k) = \ln(k_0) + \left(-\frac{E_a}{RT}\right)\frac{1}{T}. \tag{6}$$

2.10 Thermodynamic properties during the TS of juice samples

In the liquid–liquid extraction process, the transfer of solute from one liquid phase to another is a critical step that influences the extraction efficiency. To determine the Gibbs free energy change (ΔG) during this process, it is necessary to ascertain the free energies of the individual components involved.[2]

Gibbs free energy provides a deeper understanding of the energy changes occurring during the process, aiding the optimization of conditions, such as temperature, time, and sonication intensity, for achieving maximal efficiency.[9] This optimization not only enhances extraction yields but also ensures that energy is used efficiently, contributing to sustainable processing practices. The standard free energy of formation ($\Delta G°$) of a compound is a measure of the stability of that compound compared with its elements in their standard states. It can be estimated using the standard enthalpy of formation ($\Delta H°$) and standard entropy ($S°$) of the compound according to eqn (7).

$$\Delta G° = \Delta H° - T\Delta S° \tag{7}$$

The thermodynamic characteristics of the solute extraction were studied by calculating $\Delta G°$, $\Delta H°$, and $\Delta S°$. Eqn (8) presents the Gibbs free energy (thermodynamic) equation.

$$\Delta G° = -RT \ln K_e \tag{8}$$

Eqn (9) presents the van't Hoff equation, which was used to calculate $\Delta H°$ and $\Delta S°$ by combining eqn (7) and (8):

$$\ln K_e = -\frac{\Delta H°}{RT} + \frac{\Delta S°}{RT}. \tag{9}$$

where K_e, which is represented in eqn (9) as the ratio of the amount of phytochemical compound that has been extracted to the amount that remains unextracted, is the equilibrium constant for extracting the desired component.

$$K_e = \frac{EP_s}{EP_{max} - EP_s} \tag{10}$$

EP_s denotes the functional compounds extracted after 30 minutes of ultrasonic extraction at temperature T (K), while EP_{max} denotes the functional compounds retrieved after comprehensive extractions with optimal sonication time, temperature, and amplitude.

2.11 Statistical analysis

Numerous statistical parameters, including the mean square error (MSE), coefficient of determination (R^2), and chi-square (χ^2), were calculated using eqn (11)–(13), respectively.[35]

R^2 (coefficient of determination) shows the percentage of variance in the experimental data accounted for by the model. The values nearest to 1 imply a good fit. MSE (mean square error) is a quadratic estimate of the error and gives more weight to larger differences than MAE. It can be helpful in determining which models generate large outliers. χ^2 (chi-square statistic) measures the agreement between the predicted and experimental values in terms of the scale of the experimental values. Lower values correspond to better agreement of the model with the experimental data.

$$R^2 = \frac{\sum_{i=1}^{n}(EP e_i - EP\overline{e})(EP p_i - EP\overline{p})}{\sqrt{\sum_{i=1}^{n}(EP e_i - EP\overline{e})^2}\sqrt{\sum_{i=1}^{n}(EP p_i - EP\overline{p})^2}} \tag{11}$$

$$MSE = \frac{1}{n}\sum_{i=1}^{n}(e_i - p_i)^2 \tag{12}$$

$$\chi^2 = \frac{\sum_{i=1}^{n}(EP e_i - EP p_i)^2}{EP e_i} \tag{13}$$

The variables utilized in this context are e_i for experimental data, p_i for predicted values, n for the total number of observations, p for the mean value of the predicted data and e for the mean value of the experimental data. EP stands for extracted functional compounds.

3 Results and discussions

3.1 Genetic algorithm optimization of thermosonicated lapsi fruit juice

The TSLJ dataset obtained from ANN configuration (fitness function) with GA optimization was divided into three subsets: 70% for training, 15% for validation, and 15% for testing. A GA optimization graph depicting the variations in fitness values across 300 generations was obtained. The best fitness values converged around generation 200, achieving an optimal fitness value of −3.4. This indicates that the combination of 75% amplitude, 40 °C, and 60 minutes was the most effective for optimizing the 10 dependent variables. The mean fitness closely followed the best fitness, showing a consistent optimization process.[36,37]

Fig. 1 depicts the hybrid artificial neural network (ANN) and genetic algorithm (GA) system designed to optimize the thermosonication process parameters, namely, the sonication amplitude (X1), temperature (X2), and time (X3). The ANN predicted values for process outcomes, including the yield of bioactive functional compounds, were initially derived with ANN modeling utilizing the input–output relations learned from the network training. These forecasts were then combined with the genetic algorithm, which was used to train the ANN weights and biases to minimize the fitness function, maintaining the forecasted outputs within ±0.044 of the target values.[36,37] The GA used standard evolutionary procedures, such as population initialization, fitness assessment, selection, crossover, mutation, and convergence, to achieve the optimal solutions. This combined ANN–GA method improved the predictive accuracy and global optimization, and hence, it was
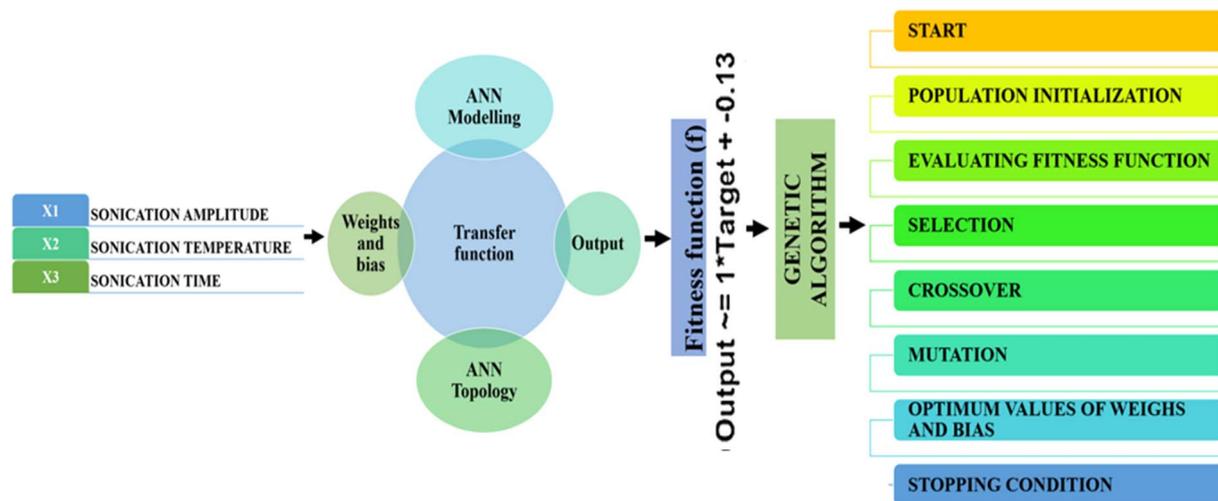
Fig. 1 Artificial neural network (ANN) and genetic algorithm (GA) framework developed to optimize the thermosonication process parameters.

very efficient for the modeling and optimization of sophisticated nonlinear processes, such as thermosonication.

Fig. 2 demonstrates the convergence pattern of the genetic algorithm (GA) for the optimization of the thermosonication parameters obtained from the ANN model-predicted values. The y-axis was plotted with fitness values, where greater negative values signified improved model fitting, and the x-axis was plotted with the number of generations.[38] The best fitness and mean fitness values initially oscillated around -3.2 with a restricted improvement. Nonetheless, there was a steep decline in the mean fitness at the 200th generation, tending towards the optimal value of -3.4. The optimum fitness was obtained at 75% amplitude, 40 °C temperature, and 60 minutes

of sonication time, as annotated on the graph. The steady low fitness variation in values thereafter proves the stability and efficacy of the optimisation process.[15]

3.2 Extraction kinetics and thermodynamics of functional compounds in LJ during TS

Table 2 shows the fitting performance of different extraction kinetic models in predicting the extraction behavior of functional compounds of thermosonicated lapsi fruit juice (TSLJ). The models were compared with respect to three important statistical parameters, namely, chi-square ($\chi^2 \times 10^{-2}$), coefficient of determination (R^2), and root mean square error (RMSE). Amongst the models that were tested, the pseudo-second-order
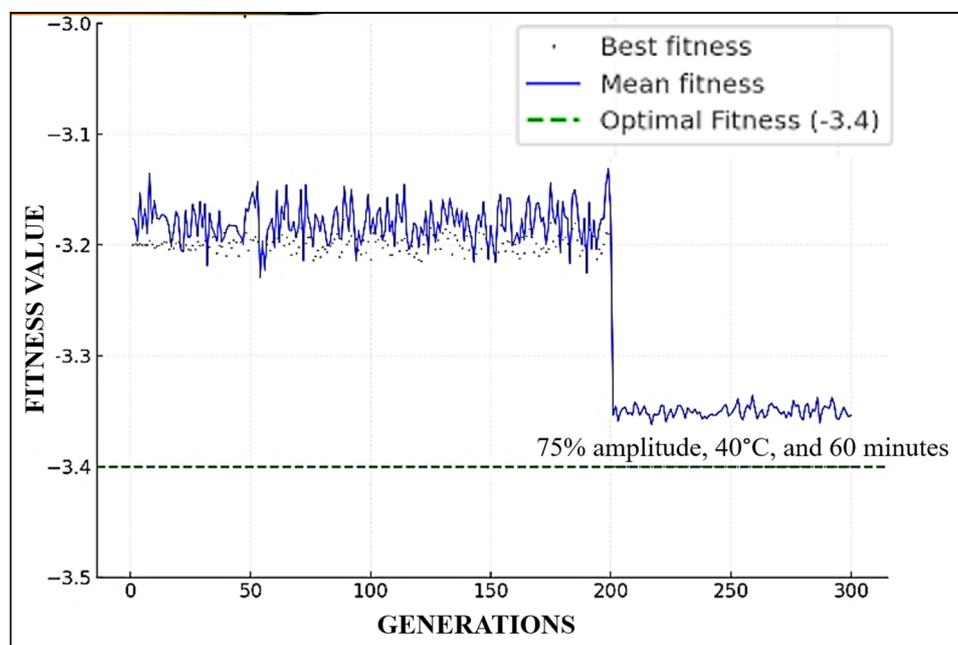

Fig. 2 GA optimization: variations in the fitness value across generations of TSLJ.

Table 2 Fittings of TSLJ (functional compounds) data to various extraction kinetic models[a]

Sl. no	Model	χ^2 ($\times 10^{-2}$)	R^2	RMSE
1	Pseudo second-order model	0.93	0.98	0.03
2	Pseudo first-order model	1.35	0.93	0.37
3	Peleg's model or hyperbolic model	1.54	0.88	0.30
4	Two-site kinetic model	1.92	0.83	0.38
5	Fick's model	2.89	0.80	0.41
6	Parabolic diffusion model	2.96	0.80	0.40

[a] Abbreviations: R^2 = Coefficient of determination; RMSE = root mean square error; χ^2 = chi-square statistics.

model fitted the best, with the lowest χ^2 (0.93), highest R^2 (0.98), and lowest RMSE (0.03) values, indicating its outstanding predictability with little deviation between the experimental and predicted values.[39] The pseudo-first-order model also fitted quite well (R^2 = 0.93) but with increased error (RMSE = 0.37). Other models, such as Peleg's, two-site, Fick's, and the parabolic diffusion models, exhibited successively worse fits, as indicated by the declining R^2 values (0.88 to 0.80) and rising χ^2 and RMSE values.[38] This comparison verifies that the extraction kinetics of functional compounds in TSLJ are most accurately explained by the pseudo-second-order model, implying that the rate-determining step could be chemisorption or square-proportional material concentration interactions.

Extraction kinetics demonstrated R^2 values of 0.99, 0.99, 0.99, and 0.99 with the lowest χ^2 values, and E_a values of 32.04, 35.23, 30.09, and 29.45 for TPC, TFC, AOA and AA, respectively. A pseudo-second-order model was employed to examine the characteristics of the model for EP_P, EP_F, EP_{AOA}, and EP_A (Fig. 3–6).[40] All the responses exhibited a rapid initial increase with rising temperature and extraction time during the early stages of the TS process.[41] This was followed by a more gradual rise, eventually plateauing towards the end of the extraction process, approximately after 55–60 minutes, reaching a saturation stage.[42]
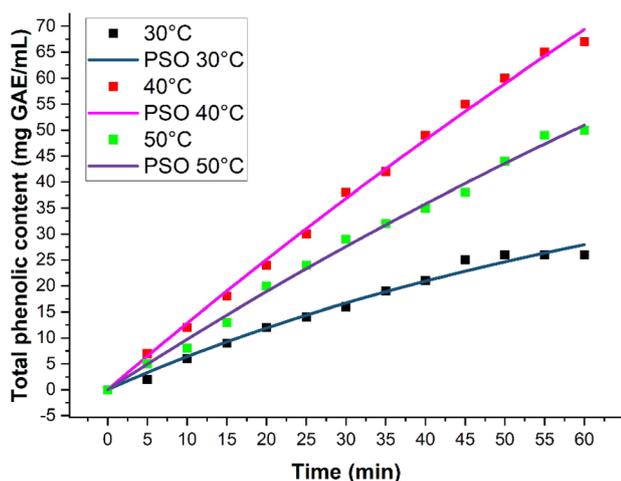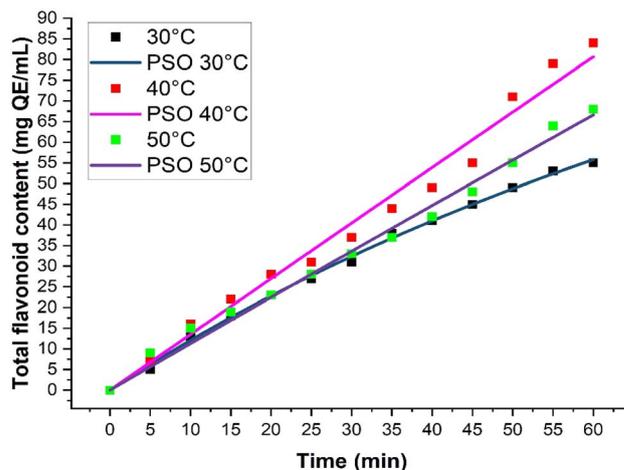

Fig. 4 Pseudo-second-order kinetic plot for the total flavonoid content extracted from TSLJ at different ultrasonication temperatures.

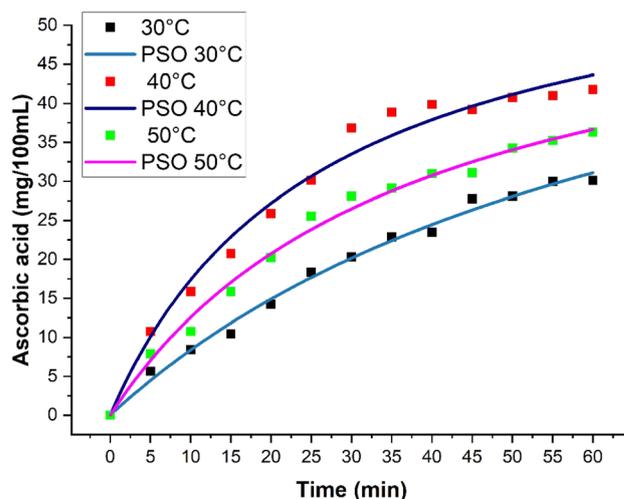**Fig. 5** Pseudo-second-order kinetic plot for the ascorbic acid content extracted from TSLJ at different ultrasonication temperatures.

Fig. 3 Pseudo-second-order kinetic plot for the total phenolic content extracted from TSLJ at different ultrasonication temperatures.
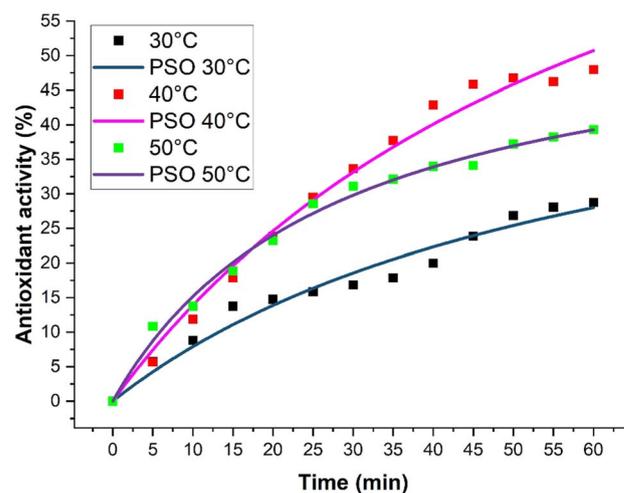

Fig. 6 Pseudo-second-order kinetic plot for the antioxidant activity of TSLJ at different ultrasonication temperatures.

3.3 Influence of thermosonication on total phenolic content

A rapid initial increase in the first 10 to 15 minutes, followed by a more gradual rise, and eventually approaching a plateau toward the end of the 60 minutes period was observed. This pattern aligned with the pseudo-second-order kinetic model, which typically describes processes where the rate of extraction is proportional to the square of the remaining unextracted compound concentration.[43] The initial rapid phase (0–15 minutes) reflected the immediate effect of thermosonication, where ultrasonic cavitation and moderate heat disrupted the plant cell matrix, releasing phenolic compounds into the juice.[38] The subsequent slower phase indicated that as more phenolics were extracted, the remaining compounds became harder to access, possibly due to the diffusion limitations or depletion of easily extractable phenolics.

TPC increased with time at all temperatures, with the maximum extraction efficiency at 40 °C, followed by 50 °C and 30 °C. This trend suggested that a moderate heat input (40 °C) increased the phenolic compound solubilization and diffusion, probably due to better cell wall permeability and penetration of the solvent, while a high heat (50 °C) resulted in partial degradation or structural rearrangement, which lowered the extractability.[44] The PSO model was a good fit for the data over all temperatures, indicating that the extraction process is governed by chemisorption phenomena, and the slowest step occurs *via* chemical bonding interaction rather than diffusion alone. The high predictability of the model highlights its applicability to modeling the extraction behavior of phenolics under various thermal conditions, which is essential for process parameter optimization in functional foods and nutraceuticals.

The graph shown in Fig. 3 depicts the pseudo-second-order kinetics of the extraction of TPC from thermosonicated lapsi juice, with a rapid initial increase at 40 °C due to ultrasonic cavitation disrupting the cell walls, followed by a plateau caused by diffusion limitations and potential thermal degradation at 50 °C, which reduces the extraction rate.[45] This reflects a mechanism where thermosonication enhances the mass transfer by breaking down the plant matrix, with temperature influencing the balance between the compound release and stability.

3.4 Influence of thermosonication on total flavonoid content

Fig. 4 provides a detailed overview of the extraction kinetics of the total flavonoid content (TFC) in terms of mg quercetin equivalents per mL (mg QE per mL) within a 60 minutes time span at three different temperatures (30 °C, 40 °C, and 50 °C), with both experimental data and respective model fittings according to the pseudo-second order (PSO) kinetic model.[20] The TFC increased consistently with time at all temperatures, indicating a time-dependent adsorption and diffusion-controlled extraction process. Among the three temperatures, 40 °C gave the highest flavonoid concentration across the entire extraction period, indicating it to be the best condition for the maximum recovery of thermolabile flavonoids, while extraction at 50 °C exhibited lower efficiency, presumably because of the thermal decomposition of flavonoid compounds.[46] The

experimental points fitted well with the pseudo-second order kinetic model, as shown by the close proximity of the model with actual data points. This is based on the argument that the rate-controlling step can include chemical sorption or valence forces through sharing or exchange of electrons, and this accurately fits when the extraction process is controlled by both external mass transfer and intramolecular interactions. The best model fit, especially at 40 °C, underscores the strength of the PSO model in predicting intricate phytochemical extraction behavior, thus serving as a reliable tool for process scale-up and optimization.[44] Overall, the graph indicates that intermediate temperatures, when combined with adequate time and PSO-based kinetic insights, can effectively optimize flavonoid extraction without inducing compound degradation, a finding that is very useful for practical uses in food, nutraceutical, and phytopharmaceutical industries.

3.5 Influence of thermosonication on ascorbic acid content

Ultrasound waves create cavitation bubbles that collapse, generating localized high-pressure and -temperature zones. This disrupts the cell walls in the food matrix, releasing more ascorbic acid into the solution, which explains the steeper initial increase in the PSO model.[46] Ascorbic acid is highly sensitive to oxygen, heat, and light, which can cause it to degrade *via* oxidation. Thermosonication alleviates this by degassing the solution, that is, by removing dissolved oxygen that would otherwise react with ascorbic acid, thus preserving its concentration over time. Thermosonication at higher temperatures (PSO 40 °C and 50 °C) accelerates this release, leading to faster ascorbic acid accumulation than that in the sample thermosonicated at 30 °C as heat aids in cell disruption and ultrasound minimizes degradation (Fig. 5).

Ascorbic acid extraction is highly dependent on time and temperature, as reflected in the graph. In the beginning, the content of ascorbic acid increased exponentially as a result of the rapid release of surface-bound molecules and effective penetration by the solvent, but later on (after 30–40 minutes), the rate of extraction tended to decrease and plateau, signifying equilibrium.[47] Temperature is an important parameter influencing this behavior, and extraction at 40 °C yielded the maximum ascorbic acid content, most probably due to increased diffusion and cell membrane permeability without much degradation. At 30 °C, the lower temperature caused retardation in mass transfer and yield, whereas at 50 °C, while diffusion might be quicker, thermal degradation of heat-sensitive ascorbic acid takes place most probably, lowering the final content.[48] These findings emphasize the need for optimizing the extraction temperature and time for maximal recovery with minimal nutrient loss, with 40 °C identified as the best extraction temperature condition in this work.

3.6 Influence of thermosonication on antioxidant activity

The plateau in antioxidant activity (around 40–50 °C) suggested that the extraction reached the maximum as the available antioxidants were fully released or only minor degradation occurred over time. Additionally, while thermosonication at 50 °

C could degrade heat-sensitive antioxidants, thermosonication at 40 °C mitigated this by using moderate heat.[49] Antioxidant activity is maximized with temperature due to enhanced solubility, diffusion, and cell disruption, while thermosonication further boosts extraction through cavitation, improved mass transfer, deaeration, and synergy with heat, leading to the highest activity in the PSO 40 °C sample (Fig. 6). The antioxidant activity of TSLJ during extraction showed definite time and temperature dependence. In the beginning, the antioxidant activity increased with time at a faster rate because bioactive compounds like phenolics and flavonoids are easily liberated from the plant matrix. Among the temperatures tested, 40 °C gave the highest antioxidant activity because there was maximum mass transfer and lowest thermal degradation of thermally sensitive antioxidants. At 30 °C, lower diffusion rates led to lower extraction efficiency, while at 50 °C, although the activity was greater than that at 30 °C, it failed to exceed the performance at 40 °C, perhaps because of the degradation of thermolabile antioxidants at high temperatures.[48] With time, the rise in activity started to taper off at all temperatures, meaning the system reached a point of equilibrium. These results indicate that 40 °C is the ideal temperature for optimum antioxidant extraction in the available time.

Both the saturation concentration (S_c) of functional compounds in the liquid extract and the pseudo-second-order rate constant (k) increased at 40 °C for all the four responses. The S_C values were in the following ranges: TPC (85.89–592.50 mg GAE per mL), TFC (126.64–200.61 mg QE per mL), AOA (57.02–108.01%) and AA (59.63–68.77 mg/100 mL). The k value ranges were found to be as follows: TPC (0.00003–0.00009 mg GAE per mL), TFC (0.00003–0.00008 mg QE per mL), AOA (0.00013–0.00061%) and AA (0.00004–0.00013 mg/100 mL) (Table 3).[50] The rise in S_c with increasing temperature could be linked to the dynamic interactions between the juice and cell matrix of the sample. The rate constant also increased with temperature, possibly due to the greater thermal energy required for the extraction of EP.[51] Escalating saturation concentrations and rate constants were observed in the extraction of antioxidant compounds, which were comparable with those of the trends observed during the microwave-assisted extraction of fenugreek leaves[52] and bioactive compounds of moringa leaves[9] within the 30–45 °C temperature range.

Data fitting to the pseudo-second-order model in this study indicates that the extraction process of bioactive compounds from LJ followed a pseudo-second-order kinetic behaviour. This finding is crucial as it provides insights into the mechanisms underlying the extraction process.[53] The high R^2 values (>0.99) obtained for TFC, AOA, TPC and AA at 40 °C suggested that the model accurately fitted with the experimental data, indicating a strong correlation between the predicted and observed values. This indicated that the extraction process was well-described by the pseudo-second-order model, and temperature had a significant impact on the extraction kinetics.[2] The activation energy values obtained for the four responses (TPC, TFC, AOA, and AA) were around 29.45 to 32.04 kJ mol^{-1}, suggesting that similar energy inputs were required for the extraction of these compounds. This implied that the extraction mechanisms of

these compounds were likely similar, possibly involving similar rate-limiting steps, such as diffusion through the cell walls or desorption from solid particles.[54] The consistency of the E_a values across different compounds further supported this hypothesis.

The increase in saturation concentration (S_c) at the temperature of 40 °C can be explained by the greater thermal energy available at 75% amplitude. This increased thermal energy helped in breaking down the cell matrix of the sample more effectively, leading to greater release of functional compounds into the liquid phase. As the temperature increased, the molecules in the sample gained more kinetic energy, which enhanced the mobility of the compounds within the sample and promoted their diffusion into the liquid phase.[33] This increased mobility and diffusion rate resulted in higher saturation concentrations of the compounds in the liquid phase. Similarly, the increase in the rate constant (k) with temperature reflected the greater thermal energy requirement for the extraction process.[9] The rate constant is a measure of the speed of the extraction process, with higher values indicating a faster rate of extraction. As the temperature increased, more thermal energy was available to drive the extraction process, leading to a higher rate constant. This suggested that the extraction process became more efficient at higher temperatures as more compounds were extracted in a shorter period due to the increased thermal energy, facilitating the breakdown of the cell matrix and release of the compounds.[9]

3.7 Thermodynamic properties of TSLJ extraction process

For TPC in the thermosonicated lapsi juice (TSLJ), the enthalpy change (ΔH) was calculated as 15.01 kJ mol^{-1}, indicating an endothermic process that required energy input to release phenolic compounds from the plant matrix. The positive entropy change ($\Delta S = 28.63$ J mol^{-1} K^{-1}) suggested increased molecular randomness during the extraction process. Gibbs free energy (ΔG) values were negative at all the temperatures, with values of -8.65 kJ mol^{-1}, -8.94 kJ mol^{-1}, and -9.23 kJ mol^{-1} at 30 °C, 40 °C, and 50 °C, respectively (Table 4). The increasingly negative ΔG values indicated that the extraction of TPC became more spontaneous at higher temperatures. This trend highlighted the favorable effect of increased temperature in facilitating the extraction of phenolic compounds during thermosonication.[13]

The enthalpy change ($\Delta H = 7.22$ kJ mol^{-1}) for TFC extraction indicated a lower energy requirement compared to TPC, reflecting the different molecular structures and extraction mechanisms of flavonoids.[55] The entropy change ($\Delta S = 25.03$ J mol^{-1} K^{-1}) also pointed to a moderate increase in system disorder. The negative ΔG values across all the temperatures, ranging from -7.57 kJ mol^{-1} to -8.07 kJ mol^{-1}, confirmed the spontaneity of the extraction process (Table 4). The more negative ΔG values at higher temperatures suggested that increasing the temperature enhanced the extraction efficiency of flavonoids in TSLJ.[56]

For AOA, the thermodynamic parameters revealed a significantly higher enthalpy change ($\Delta H = 15.64$ kJ mol^{-1}) compared

Table 3 The pseudo-second-order model parameters for the optimized extraction conditions of functional compounds from TSLJ (75% amplitude) at different temperatures[a]

Response	Temperature	k	S_C	χ^2 ($\times 10^{-2}$)	R^2	RMSE	E_a (kJ mol^{-1})
TPC	30 °C	9×10^{-5}	85.89 ± 3.03	1.19	0.98	0.30	32.04
	40 °C	3×10^{-5}	592.50 ± 1.81	1.47	0.99	0.33	
	50 °C	8×10^{-5}	334.39 ± 1.44	1.44	0.99	0.33	
TFC	30 °C	3×10^{-5}	126.64 ± 2.84	1.16	0.98	0.29	35.23
	40 °C	5×10^{-5}	200.61 ± 44.66	0.12	0.99	0.09	
	50 °C	8×10^{-5}	160.13 ± 3.85	1.04	0.98	0.28	
AOA	30 °C	2×10^{-4}	57.02 ± 1.25	2.83	0.98	0.46	30.09
	40 °C	1×10^{-4}	108.01 ± 1.51	1.30	0.99	0.31	
	50 °C	6×10^{-4}	57.17 ± 1.92	3.66	0.96	0.53	
AA	30 °C	4×10^{-5}	62.29 ± 2.92	1.21	0.98	0.30	29.45
	40 °C	1×10^{-4}	68.77 ± 2.10	0.78	0.99	0.24	
	50 °C	7×10^{-5}	59.63 ± 2.40	3.57	0.98	0.52	

[a] Abbreviations: Temperature 30, 40 and 50 °C, TPC = total phenolic content; TFC = total flavonoid content; AOA = antioxidant activity; AA = ascorbic acid; R^2 = Coefficient of determination; RMSE = root mean square error; χ^2 = chi-square statistic; k = pseudo-second-order rate constant; S_C = saturation concentration; and E_a = activation energy.

Table 4 Thermodynamic parameters for the extraction of TPC, TFC, AOA and AA from TSLJ[a]

Response	Temperature	ΔH (kJ mol^{-1})	ΔS (J mol^{-1} K^{-1})	ΔG (kJ mol^{-1})
TPC	30 °C	15.01	28.63	−8.65
	40 °C			−8.94
	50 °C			−9.23
TFC	30 °C	7.22	25.03	−7.57
	40 °C			−7.82
	50 °C			−8.07
AOA	30 °C	15.64	57.23	−17.32
	40 °C			−17.89
	50 °C			−18.46
AA	30 °C	5.44	18.03	−5.45
	40 °C			−5.63
	50 °C			−5.81

[a] Abbreviations-ΔH: Enthalpy; ΔS: Entropy; ΔG: Gibbs free energy.

with TFC, indicating a higher energy requirement for the release of antioxidant compounds. The entropy change ($\Delta S = 57.23$ J mol^{-1} K^{-1}) was notably higher, suggesting a substantial increase in molecular disorder during the extraction process.[57] Gibbs free energy (ΔG) values were strongly negative, ranging from −17.32 kJ mol^{-1} to −18.46 kJ mol^{-1}, indicating a highly favorable and spontaneous extraction process (Table 4). The increasingly negative ΔG values with rising temperature affirmed that higher temperatures promoted the efficient extraction of antioxidant compounds during thermosonication.[58]

For ascorbic acid, the enthalpy change ($\Delta H = 5.44$ kJ mol^{-1}) was the lowest among all the responses, indicating minimal energy requirements for its extraction. The entropy change ($\Delta S = 18.03$ J mol^{-1} K^{-1}) reflected a modest increase in molecular randomness. The negative ΔG values, ranging from −5.45 kJ mol^{-1} to −5.81 kJ mol^{-1}, confirmed the spontaneity of the extraction process (Table 4).[59] However, the smaller

magnitude of ΔG compared with TPC, TFC, and AOA suggested that the spontaneity of ascorbic acid extraction was less temperature-dependent, likely due to its inherent solubility and stability under thermosonication conditions.

The thermodynamic parameters for TSLJ demonstrated that the extraction of TPC, TFC, AOA, and AA during thermosonication was spontaneous at all the studied temperatures, with increasingly favorable ΔG values at higher temperatures. TPC and AOA exhibited higher ΔH, indicating greater energy requirements, while TFC and AA required comparatively less energy for extraction. The positive ΔS values across all the responses suggested that the thermosonication process increases the molecular randomness, likely due to the breakdown of cellular structures and enhanced mass transfer.[60] These results highlighted the efficacy of thermosonication in facilitating the extraction of bioactive compounds from lapsi juice, with temperature playing a crucial role in optimizing the yield and efficiency.

4 Conclusion

This study highlights the effectiveness of thermosonication in extracting functional compounds by assessing the total phenolic content (TPC), total flavonoid content (TFC), antioxidant activity (AOA), and ascorbic acid (AA) content from lapsi fruit juice. The process kinetics followed a pseudo-second-order model, demonstrating high R^2 values (0.99743–0.99856) and low χ^2 values, indicating a precise fit. Activation energy (E_a) ranged from 29.46 to 35.23 kJ mol^{-1}, confirming its temperature dependency and moderate energy requirement. The thermodynamic parameters revealed spontaneous extraction at all temperatures, with negative Gibbs free energy (ΔG) values that became increasingly favorable as temperature increased. Enthalpy (ΔH) and entropy (ΔS) changes suggested the process was endothermic, with enhanced molecular randomness promoting the extraction efficiency. The findings demonstrate that thermosonication is a sustainable and efficient technique

for maximizing bioactive compound recovery, particularly at optimized conditions (75% amplitude, 40 °C temperature, and 60 minutes of sonication time), with significant potential in industrial and nutritional applications. It provides a robust framework for scale-up, emphasizing the need for precise temperature and time management to preserve quality. The adaptability of this approach to lapsi fruit suggests its broader applicability to other underutilized species, paving the way for sustainable food processing innovations. Future efforts could refine these parameters further and explore additional fruits to maximize the potential of TS in delivering nutrient-rich products.

Author contributions

Puja Das: conceptualization, formal analysis, investigation, data curation, methodology, validation, writing-original draft. Prakash Kumar Nayak: conceptualization, supervision, validation, review, and editing. Radha krishnan Kesavan: conceptualization, supervision, validation, writing review and editing, formal analysis, data curation. All authors reviewed the results and agreed to the published version of the manuscript.

Conflicts of interest

The authors declare no conflicts of interest.

Data availability

All the data generated or analyzed during this study are included in the manuscript.

References

1 Z. Ahmed, M. F. Manzoor, N. Begum, A. Khan, I. Shah, U. Farooq, R. Siddique, X. A. Zeng, A. Rahaman and A. Siddeeg, *Processes*, 2019, **7**, 518.

2 X. Guo, S. Liu, Z. Wang and G. Zhang, *Biochem. Eng. J.*, 2022, **177**, 108227.

3 P. Singh, L. Bilyeu and K. Krishnaswamy, *LWT–Food Sci. Technol.*, 2022, **166**, 113760.

4 S. Gogoi, P. Das, P. K. Nayak, K. Sridhar, M. Sharma, T. P. Sari, R. krishnan Kesavan and M. Bhaswant, *Foods*, 2024, **13**, 497.

5 S. K. Dutta, Vanlalhmangaiha, R. S. Akoijam, Lungmuana, T. Boopathi and S. Saha, *J. Food Meas. Charact.*, 2018, **12**, 2503–2514.

6 S. Mann, D. Chakraborty and S. Biswas, *Food Biosci.*, 2022, **47**, 101609.

7 P. Das, P. K. Nayak and R. krishnan Kesavan, *Food Chem. Adv.*, 2022, **1**, 100144.

8 S. J. Granella, T. R. Bechlin, D. Christ, S. R. Coelho Machado, C. C. Triques and E. A. da Silva, *J. Appl. Res. Med. Aromat. Plants*, 2023, **34**, 100484.

9 R. Albarri and S. Şahin, *Biomass Convers. Biorefin.*, 2023, **13**, 7919–7926.

10 B. C. Steffens, B. N. Segala, E. H. Tanabe, C. A. Ballus and D. A. Bertuol, *Food Bioprod. Process.*, 2024, **143**, 158–169.

11 M. Sharma and K. K. Dash, *Innovative Food Sci. Emerging Technol.*, 2022, **75**, 102913.

12 F. Hou, S. Song, S. Yang, Y. Wang, F. Jia and W. Wang, *Foods*, 2024, **13**, 1408.

13 S. M. B. Hashemi, R. Roohi and E. Abedi, *Ultrason. Sonochem.*, 2024, **104**, 106820.

14 P. Das, P. K. Nayak and R. krishnan Kesavan, *J. Food Process Eng.*, 2024, **47**, e14682.

15 P. Das, P. K. Nayak and R. krishnan Kesavan, *Prep. Biochem. Biotechnol.*, 2025, **55**, 171–186.

16 P. Das, P. K. Nayak, B. Stephen Inbaraj, M. Sharma, R. krishnan Kesavan and K. Sridhar, *Foods*, 2023, **12**, 3723.

17 N. Singh, S. Kumar and D. S. Patle, *Sep. Purif. Technol.*, 2025, **359**, 130681.

18 E. Ikharia, M. Ekpenyong, D. Ubi, E. Akwagiobe, U. Ben, A. Asitok, A. Akpan and S. Antai, *J. Food Sci. Technol.*, 2024, 1–14.

19 H. Chutia, F. Begum, S. Rohilla and C. L. Mahanta, *Int. J. Food Eng.*, 2024, **20**, 463–474.

20 Y. wei Ji, G. wei Rao and G. fa Xie, *Prep. Biochem. Biotechnol.*, 2022, **52**, 1060–1068.

21 Y. Xiang, Z. Liu, Y. Liu, B. Dong, C. Yang and H. Li, *Ultrason. Sonochem.*, 2024, **111**, 107079.

22 A. S. M. Sayem, T. Ahmed, M. U. K. Mithun, M. Rashid and M. R. Rana, *J. Agric. Food Res.*, 2024, **18**, 101312.

23 H. Che, R. Zhang, X. Wang, H. Yu, X. Shi, J. Yi, J. Li, Q. Qi, R. Dong and Q. Li, *Ultrason. Sonochem.*, 2024, **111**, 107083.

24 M. Peleg, *Food Eng. Rev.*, 2024, **16**, 163–178.

25 M. Askarizadeh, N. Esfandiari, B. Honarvar, S. A. Sajadian and A. Azdarpour, *ChemBioEng Rev.*, 2023, **10**, 1006–1049.

26 J. P. Vareda, *J. Mol. Liq.*, 2023, **376**, 121416.

27 G. V. S. Bhagya Raj and K. K. Dash, *Comput. Electron. Agric.*, 2020, **178**, 105814.

28 A. Ali, X. Y. Lim, C. H. Chong, S. H. Mah and B. L. Chua, *Sep. Sci. Technol.*, 2018, **53**, 2192–2205.

29 I. Das and A. Arora, *Food Hydrocolloid*, 2021, **120**, 106931.

30 Y. Tao, Z. Zhang and D. W. Sun, *Ultrason. Sonochem.*, 2014, **21**, 1461–1469.

31 N. S. Yadav and K. Mukherjee, *Numer. Algorithms*, 2024, **96**, 925–973.

32 P. Hobbi, O. V. Okoro, C. Delporte, H. Alimoradi, D. Podstawczyk, L. Nie, K. V. Bernaerts and A. Shavandi, *Bioresour. Bioproces*, 2021, **8**, 1–14.

33 F. Galgano, R. Tolve, T. Scarpa, M. C. Caruso, L. Lucini, B. Senizza and N. Condelli, *Foods*, 2021, **10**, 1810.

34 Sucheta, N. N. Misra and S. K. Yadav, *Food Hydrocolloid*, 2020, **102**, 105592.

35 G. Patel, A. Patra, S. Abdullah and M. Dwivedi, *Appl. Food Res.*, 2022, **2**, 100080.

36 K. Nwosu-Obieogu, G. W. Dzarma, C. Linus, O. Nwosu and C. Udemgba, *Proc. Natl. Acad. Sci., India, Sect. B*, 2024, **94**, 1041–1049.

37 W. Liao, J. Shen, S. Manickam, S. Li, Y. Tao, D. Li, D. Liu and Y. Han, *Food Chem.*, 2023, **405**, 134982.

38 P. Das, P. K. Nayak, M. Sharma, V. B. Raghavendra, R. K. Kesavan and K. Sridhar, *J. Food Process. Preserv.*, 2024, **2024**, 5559422.

39 P. Das, P. K. Nayak and R. krishnan Kesavan, *Prep. Biochem. Biotechnol.*, 2025, **55**, 171–186.

40 S. Giri, K. Kumar Dash, G. V. S. Bhagya Raj, B. Kovács and S. Ayaz Mukarram, *Ultrason. Sonochem.*, 2024, **102**, 106759.

41 P. Sun, W. Yang, T. Sun, Y. Tang, M. Li, S. Cheng and G. Chen, *Food Res. Int.*, 2024, **191**, 114674.

42 K. Guo, X. Wu, F. Zhang, Y. Cao, Z. Tan, S. Xiao and L. Wu, *Molecules*, 2024, **29**, 3423.

43 A. Nicolescu, M. Babotă, L. Zhang, C. I. Bunea, L. Gavrilaș, D. C. Vodnar, A. Mocan, G. Crișan and G. Rocchetti, *Antioxidants*, 2022, **11**, 1123.

44 P. Das, P. K. Nayak and R. krishnan Kesavan, *Sustainable Food Technol.*, 2024, **2**, 790–805.

45 M. Sharma and K. K. Dash, *Innovative Food Sci. Emerging Technol.*, 2022, **75**, 102913.

46 A. Patra, S. Abdullah and R. C. Pradhan, *J. Food Process. Preserv.*, 2022, **46**, e16317.

47 P. R. More and S. S. Arya, *Chem. Eng. Process.*, 2024, **202**, 109839.

48 S. M. B. Hashemi, R. Roohi and E. Abedi, *Ultrason. Sonochem.*, 2024, **104**, 106820.

49 M. Zhang, Y. Li, X. xiang Shuai, J. Qiao, C. bin Wei, F. yue Ma, Y. han Zhang and L. qing Du, *LWT–Food Sci. Technol.*, 2023, **189**, 115552.

50 R. Bahrami, B. Ebrahimi, F. Hameed Awlqadr, M. Rouhi, G. Paimard, Z. Sarlak, M. Fallah, K. Khalghimanesh and R. Mohammadi, *Food Control*, 2025, **168**, 110880.

51 R. Ezzati, S. Ezzati and M. Azizi, *Vacuum*, 2024, **220**, 112790.

52 M. K. I. Khan, Y. M. Ghauri, T. Alvi, U. Amin, M. I. Khan, A. Nazir, F. Saeed, R. M. Aadil, M. T. Nadeem, I. Babu and A. A. Maan, *Food Sci. Technol.*, 2021, **42**, e56020.

53 R. Ezzati, M. Azizi and S. Ezzati, *Vacuum*, 2024, **222**, 113018.

54 M. Dabbour, H. Jiang, B. K. Mintah, H. Wahia and R. He, *Innovative Food Sci. Emerging Technol.*, 2021, **74**, 102824.

55 M. E. Mahmoud, G. F. El-Said, G. A. A. Ibrahim and A. A. S. Elnashar, *Biomass Convers. Biorefin.*, 2024, **14**, 14725–14743.

56 U. Bello, N. A. Amran, M. S. H. Ruslan and H. Adamu, *Biomass Convers. Biorefin.*, 2024, **14**, 15893–15908.

57 B. Z. Ek, E. Kurtulbaş and S. Şahin, *Biomass Convers. Biorefin.*, 2024, **14**, 8385–8393.

58 A. Lopes Ferrari, M. Carolina Sérgi Gomes, A. Caroline Raimundini Aranha, S. Marques Paschoal, G. de Souza Matias, L. Mario de Matos Jorge and R. Oliveira Defendi, *Sep. Purif. Technol.*, 2024, **337**, 126310.

59 A. M. Alotaibi, J. S. Alnawmasi, N. A. H. Alshammari, M. A. Abomuti, N. H. Elsayed and M. G. El-Desouky, *Int. J. Biol. Macromol.*, 2024, **274**, 133442.

60 C. M. Agu, C. C. Orakwue, O. N. Ani, M. P. Chinedu, C. H. Kadurumba and I. E. Ahaneku, *Sustain. Chem. Environ*, 2024, **5**, 100064.